Effect of the pearlite content of ferritic cast iron material on the crack resistance behaviour under dynamic load

Peter Trubitz[1], Hans-Peter Winkler[2,], Roland Hüggenberg[2], Annette Ludwig[1,*], Gerhard Pusch[1]**

[1]Technical University Bergakademie Freiberg, Freiberg, Germany
[2]Gesellschaft für Nuklear-Service mbH, Essen, Germany
[*]Corresponding author: ludwig@ww.tu-freiberg.de
[**]Corresponding author: hans-peter.winkler@gns.de

Abstract
The factor of safety against rupture of castings subject to high-strength loads, such as transport and pressure vessels as well as windmill components, is assessed taking into account fracture mechanical characteristic values for the static, cyclic and dynamic load condition. The experimental investigation of dynamic crack initiation values with regard to cast iron-specific aspects was the subject of a contribution at the 12th ICF in Ottawa.

Continuing the examination, the contribution on hand describes the effect of the microstructure on the mechanical and fracture-mechanic properties of ferritic and ferrite-pearlite cast iron materials at low temperatures. The strength and sensibility to brittle fracture are conventionally evaluated by applying the characteristic values of the tensile test or the notched bar impact test. During the recording of the notched bar impact work-temperature curves in the temperature range of 180 °C to -60 °C, the transition temperature curves are defined by comparing various criteria. The dynamic crack initiation values at -40 °C are determined via the recording of cracking resistance curves (J integral concept). In addition, via the determination of the crack arrest toughness K_{Ia} at 50 mm thick CCA samples, the crack arrest behaviour is controlled in the temperature range of -40 °C to -80 °C.

Keywords Cast iron, perlite content, crack resistance behavior, dynamic loading

1 Introduction

Resulting from various solidification and cooling conditions, microstructures may develop distinguishing themselves clearly with regard to the graphite morphology and pearlite content. Using the example of ferritic or ferrite-pearlite ferritic cast iron materials, the contribution on hand describes their effect on the mechanical and fracture-mechanic properties at low temperatures.

2 Materials

The examinations were performed on ductile ferritic cast iron materials with various pearlite content (Fig. 1), designated in the following GJS (4) and GJS (29).

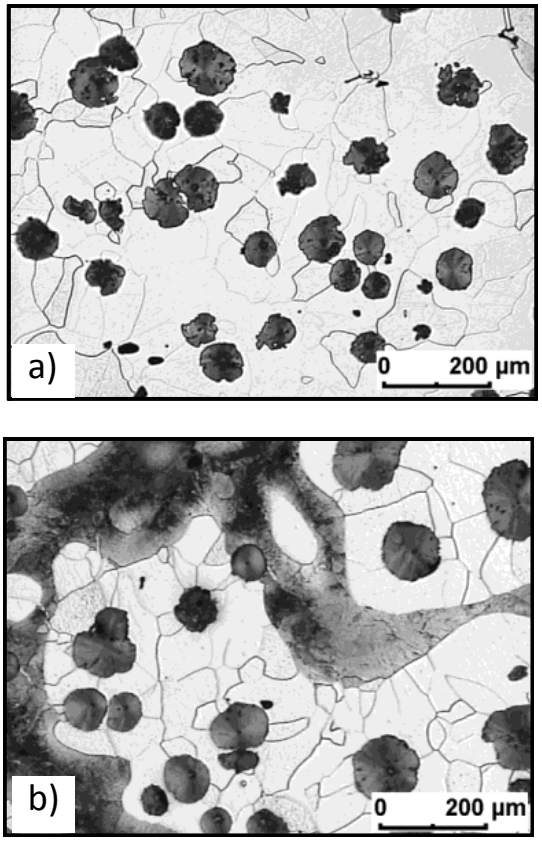

Microstructure parameters:

Diameter of the graphite particles: 63 µm
Ferrite grain size: 62 µm
Particle separation: 88 µm
Form factor: 0.71
Number of particles: 47 mm^{-2}

Pearlite content: 4 %

Microstructure parameters:

Diameter of the graphite particles: 69 µm
Ferrite grain size: 62 µm
Particle separation: 102 µm
Form factor: 0.74
Number of particles: 32 mm^{-2}

Pearlite content: 29 %

Figure 1: Microstructure and microstructure parameters a) GJS (4), b) GJS (29)

3 Mechanical characteristic values

The characteristic values of the tensile test were always determined on three tensile tests according to DIN EN 10 002 at RT and taking into account the special application at -40 °C (Tab. 1).

Table 1: Mechanical characteristic values and hardness values

Material	Temperature °C	$R_{p0.2}$ MPa	R_m MPa	A %	Z %	E GPa	ν	HBW 2.5/187.5
GJS(4)	RT	245	367	12	13	172	0.28	137
	-40	273	393	10	11			
GJS(29)	RT	284	424	11	12	174	0.28	163
	-40	315	427	5	5			

The notched bar impact test according to DIN EN 10 045-1 was performed with ISO-V samples (10x10x55 mm) using a 300 J pendulum striking mechanism in a temperature range of 180 °C to -60 °C, whereby at each temperature three samples were tested. Following the determination of the notched bar impact work used KV and the lateral expansion LE the approximation of the KV-T or LE-T-curves is performed according to Eq. 1

$$KV, LE = X + Y \tanh \frac{T - T_0}{Z} \quad (1)$$

The transition temperature T_t was determined by calculating the KV-T or LE-T curves at 0.5 (KV_{max} + KV_{min}) or 0.5 (LE_{max} + LE_{min}), Tab. 2.

Table 2: Characteristic values of the notched bar impact test

	Parameter equation (1)				KV (RT)	KV (-40 °C)	T_t^{KV}
Material	T_0 °C	X -	Y -	Z -	J	J	°C
GJS (4)	-2.2	10.54	6.14	28.30	17	5	-2
GJS (29)	66.6	12.44	8.24	42.56	7	5	67
Material	T_0 °C	X -	Y -	Z -	LE (RT) mm	LE (-40 °C) mm	T_t^{LE} °C
GJS (4)	3.3	0.27	0.25	38.03	0.43	0,10	3
GJS (29)	66.6	0.32	0.27	55.54	0.18	0,07	67

The differently determined transition temperatures show a good correlation.

4 Fracture mechanical characteristic values

The static fracture mechanical characteristic values of the J integral concept at -40 °C (Tab. 3) were determined at 20% side grooved SENB-samples (10x20x120 mm) according to ESIS P2-92 applying the compliance method, and the J_R curves approximated with the extended power approach, Eq. 2

$$\mathrm{J} = \mathrm{A}(\Delta\mathrm{a} + \mathrm{B})^{\mathrm{C}} \quad (1)$$

The physical crack initiation values $J_{i/BL}$ are determined with the J_R curve at the point of intersection of the blunting line according to Eq. 3

$$J = 3.75 \cdot R_m \cdot \Delta a \quad (2)$$

The technical crack initiation values $J_{0.2}$ are determined at Δa = 0.2 mm (Fig. 2). The conversion of the J values into the respective characteristic values of the K concept is performed via the elastic constants according Eq. 4 to.

$$K(J) = \left[\frac{J \cdot E}{1 - \nu^2}\right]^{1/2} \quad (4)$$

Apart from the determination of the crack initiation values, the increase in the cracking resistance curve distinguishes the material resistance against a constant crack propagation, which can be defined as T module (tearing modulus) according to Eq. 5

$$T^J = \frac{dJ}{da} \cdot \frac{E}{\left(R_{p0.2}\right)^2} \quad (3)$$

Here, the T^J module is quantified during the applied nonlinear curve adjustment according to the Eq. 5 via the increase of the secant in the range of Δa = 0.2 mm to Δa = 1 mm.

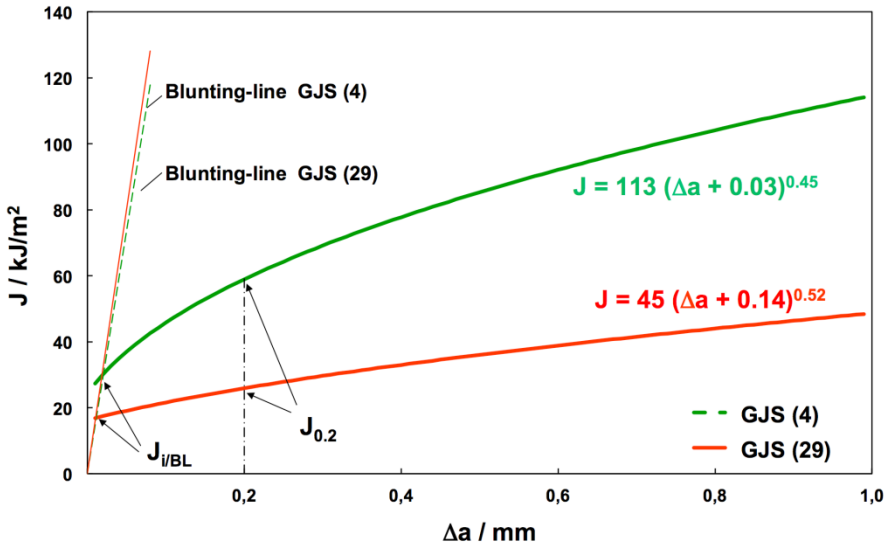

Figure 1: Static J_R curves at -40 °C

Table 3: Static fracture toughness characteristic values of the J integral concept at -40 °C

Material	A -	B -	C -	$J_{i/BL}$ kJ/m²	$J_{0.2}$ kJ/m²	K ($J_{i/BL}$) MPa√m	T^J
GJS (4)	113	0.03	0.45	28	59	73	162
GJS (29)	46	0.14	0.52	16	26	55	50

The experimental investigation of the dynamic cracking resistance curves of the J-integral-concept (J_{dR}-curves) was carried out on 20 % side-grooved SENB samples (10x10x55 mm) with fatigue cracking according to the "low-blow"-technique using an instrumented pendulum. Thereby, six to eight samples in the range $2.8 \cdot 10^4$ MPa√m/s ≤ $\dot{K}$ ≤ $5.7 \cdot 10^4$ MPa√m/s were stressed, the J_d values were determined via the calculated dynamic force-distance diagrams and the Δa values were determined on the fracture surfaces of the samples. Testing procedure and evaluation were performed in adaptation to ESIS P2-92. Contrary to the static load, the stable ductile crack propagation for the dynamic load is replaced with a stable cleavage-faced crack propagation. The resulting material-specific aspects with regard to recording, evaluation and definition of the dynamic crack initiation values have been described in [1] and [2]. The determined J_{dR}-curves or the characteristic values derived from these are shown in Fig. 3 and Tab. 4. Occurring "pop-in"-effects can be attributed to pearlite islands or graphite degenerations. For GJS (29) no experimental determination of a J_d-Δa-curve was possible at -40 °C, since only "pop-in" effects occurred. They are to be attributed to the increased pearlite content and are shown in Table 4 as J_{dc} values. The range of the J_{dc} values corresponds with the size and/or the number of the pearlite islands in front of the crack tip.

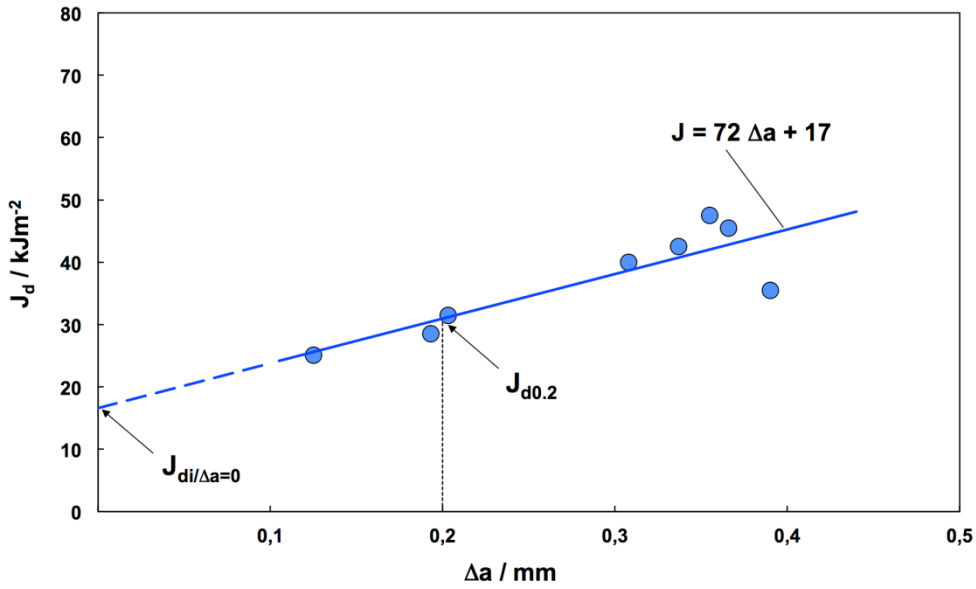

Fig. 2: Dynamic J_{dR} curve of the GJS(4) at -40 °C

Table 4: Dynamic fracture toughness characteristic values of the J integral concept at -40 °C

Material	$J_{di/\Delta a=0}$ kJ/m²	$J_{d0.2}$ kJ/m²	$K(J_{di/\Delta a=0})$ MPa√m	T_d^J	J_{dc} kJ/m²	$K(J_{dc})$ MPa√m
GJS (4)	17	31	56	64	22[1)]	64
GJS (29)	-	-	-	-	10[2)]	34

[1)]…Mean value of 6 samples with J_{dc}^{min} = 16 kJ/m² and J_{dc}^{max} = 27 kJ/m²
[2)]…Mean value of 10 samples with J_{dc}^{min} = 6 kJ/m² and J_{dc}^{max} = 14 kJ/m²

While the dynamic fracture toughness distinguishes the material resistance against instable crack propagation for impact load, the crack arrest toughness K_{Ia} evaluates the ability of the material to trap a crack propagating at high speed. A crack arrest presents a special case of an instable crack propagation aiming to secure components with high requirement on the safety against fracture on the material and / or load side so that instably propagating cracks as a result of overstress and / or embrittlement on the material side are trapped again before a catastrophic failure occurs. The crack arrest toughness K_{Ia} is determined according to ASTM E 1221-06 on 50 mm thick CCA-samples in the temperature range of -40 °C to -80 °C.

A temperature equalisation is possible via the cooling system of the base plate, on which the CCA-sample rests. After setting the test temperature, the sample is loaded with 5 to 10 mm/min via a wedge firmly connected to the crosshead of the testing machine. Thus, this is pressed into the divided jaws located in the bore, and the sample is loaded until, starting at the notched welding bead, instable crack propagation occurs (Fig. 4).

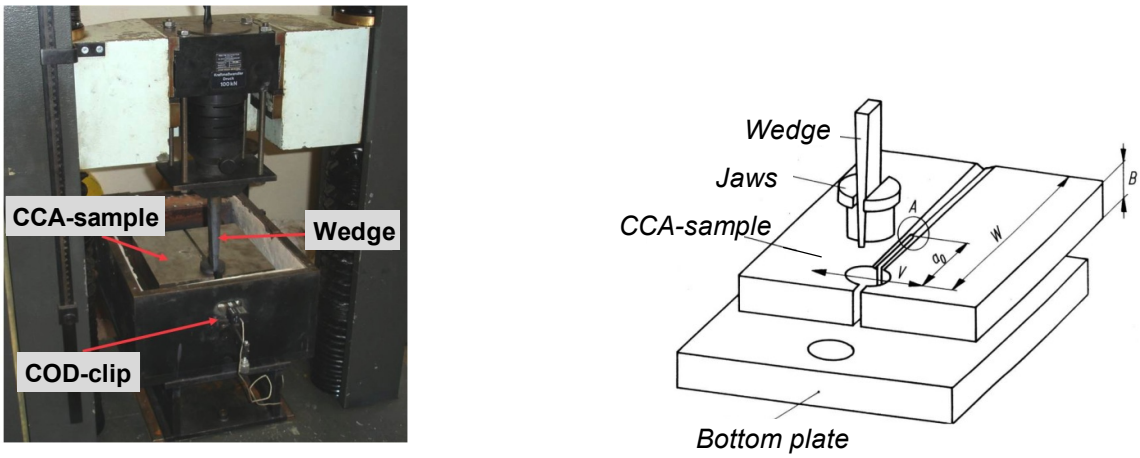

Fig. 3: Test set-up and transversal wedge load of the CCA-samples according to ASTM E 1221-06 (A: brittle build-up welding with notch)

During the test, the force and the notch opening (COD clip) are registered. An abrupt notch opening with a simultaneous reduction of force indicates an instable crack propagation. Details on the test evaluation are specified in ASTM E 1221-06. To this end, with regard to the validity criteria concerning the minimum and maximum crack length as well as the verification of the required minimum sample thickness B implementing the level elongation state according to

$$B \geq 2.5 \left(\frac{K_{Ia}}{R_{dp0.2}} \right)^2 \tag{6}$$

It must be taken into account that this requires knowledge of the dynamic yield strength $R_{dp0.2}$. The determination of $R_{dp0.2}$ for ferritic cast iron materials is possible via the Arrhenius equation (Eq. 7) describing the dependence of the dynamic yield strength of the elongation rate $\dot{\varepsilon}$ and the temperature according to

$$R_{dp0.2} = \sigma_i + \sigma_0^* \left[1 - \frac{k \cdot T \cdot ln \, {\dot{\varepsilon}_0}/{\dot{\varepsilon}}}{\Delta G_0} \right]^m \tag{7}$$

The parameters of the Arrhenius equation ($\dot{\varepsilon}_0 = 8.68 \cdot 10^8$/s, σ_i = 212 MPa, σ_0^* = 621 MPa, $\Delta G_0 = 2.2 \cdot 10^{-19}$ J, m = 3.43) determined within extensive examinations [3] of 15 batches at T = -80 °C and $\dot{\varepsilon}$ = 1/s result in a value for $R_{dp0.2}$ = 422 MPa. The specified elongation rate corresponds with $\dot{K} = dK/dt$ values between 10^4 MPa√m/s and 10^5 MPa√m/s existing during impact bending tests determining dynamic K_{Id} values. For ferrite-pearlite cast iron materials, the value $R_{dp0.2}$ = 385 MPa determined in [4] for $\dot{\varepsilon}$ = 1/s and -40 °C can be used. The crack-arrest tests performed on 50 mm thick CCA-samples in the temperature range of -40 °C to -80 °C show that due to the failure to achieve the "minimum crack length" required by the standard, at -40 °C

and -60 °C no valid K_{Ia} values can be determined. The cause is the still available high crack initiation toughness. This also applies to the ferritic as well as the ferrite-pearlite cast iron. The conditions for the check of the level elongation state are only met at -80 °C, and valid K_{Ia} values can be determined, which are in the range 44 MPa√m ≤ K_{Ia} ≤ 61 MPa√m. The crack propagation occurs at -80 °C, also within the fracture surface area of the crack-arrest, exclusively cleavage-faced, whereby crack trapping can be attributed material-specific to the energy-dissipative effect of the graphite particles.

5 Summary

A summarising evaluation of the effect of the pearlite content on the mechanical and fracture mechanical characteristic values is performed based on a graphical representation of the characteristic values determined (Fig. 5 to Fig. 7). In addition to the expected work-hardening with declining temperature and higher pearlite content, only with higher pearlite content and -40 °C a significant decrease of the plasticity occurs, i.e. a more than 50 % decrease of the fracture elongation A or the percentage reduction of fracture Z (Fig. 5).

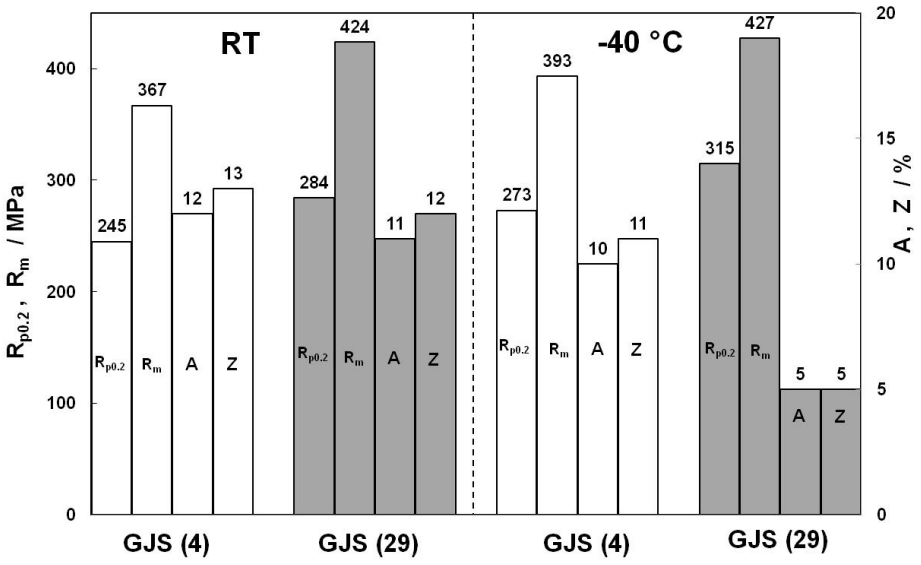

Figure 5: Mechanical characteristic values of the tensile test

With a sudden load, the increased pearlite content leads to a significant decrease in toughness, as resulting from the course of the KV-T curves (Fig. 6a) and the notched bar impact work used KV at RT as well as the transition temperature T_t (Fig. 6b). At -40 °C, both materials are located in the lower position of the KV-T-curve.

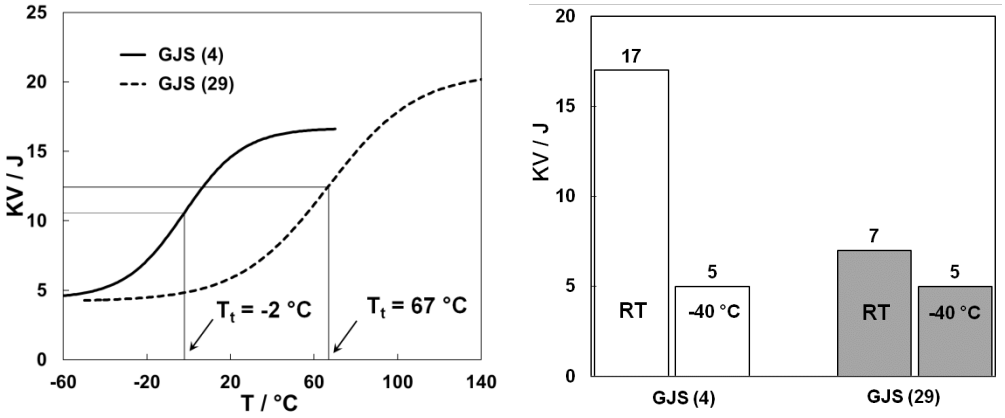

a) KV-T curves b) KV values (RT and -40 °C)

Figure 4: Mechanical characteristic values of the notched bar impact test

It results from the comparison of static fracture-toughness values at -40 °C that the increased pearlite content leads to a significant reduction of the material resistance against crack initiation ($J_{i/BL}$, $J_{0.2}$) and ductile stable crack propagation (T^J). As the dynamic fracture-toughness values of the GJS (4) show, a shock load at this temperature leads, due to the cleavage-faced stable crack propagation, to a significant decrease of the crack resistance behaviour (Fig. 7). With these loading conditions, the effect of the pearlite becomes also apparent with the occurrence of "pop-in"-effects, occasionally with GJS (4) and exclusively with GJS (29).

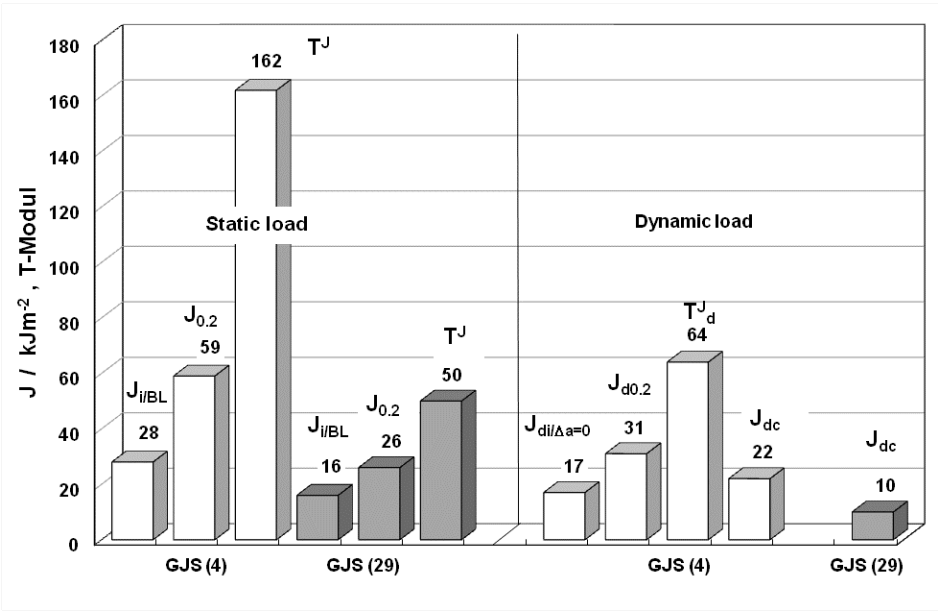

Fig. 5: Fracture mechanical characteristic values for static and dynamic load (-40 °C)

The K_{Ia} values determined at -80 °C are evaluated via the allocation to the reference curve on hand (lower-bound curves) to the temperature-dependent course of the K_{Ia} values (Fig. 8). There only tends to be an effect noticeable with regard to the increased pearlite content.

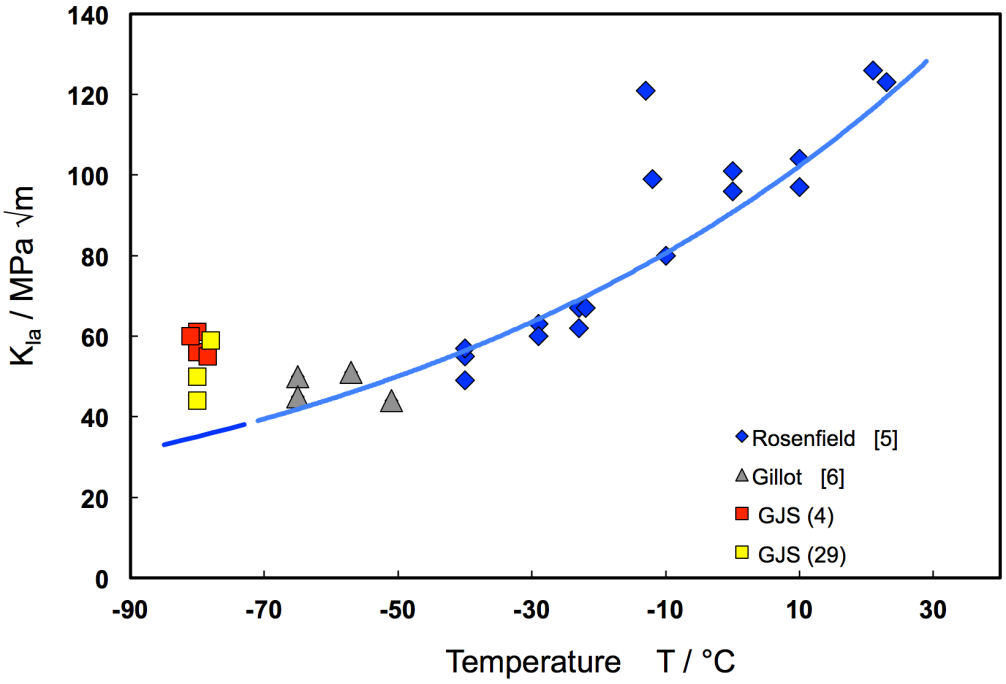

Figure 6: K_{Ia}-values for ferritic cast iron as a function of the temperature

According to [5], the determination of valid K_{Ia} values at ferritic cast iron in the temperature range of -40 °C to 20 °C is only possible by means of a duplex-arrest sample, to which a hardened steel (AISI 4340) as the crack starter is connected via a work intensive heat-treated electron-beam welded connection with the GJS-400 test specimen. In this combination, the crack does not start in a brittle build-up welding according to (Fig 4), but inside the hardened steel and runs into the cast iron at high speed. Thus, the determination of the K_{Ia} values can be implemented even at the higher temperatures specified in Fig. 7. The temperature-dependent course of the K_{Ia} values integrates the values listed in [6] as well as the K_{Ia} values determined here at -80 °C. Based on the temperature-dependent course of the K_{Ia} values, an estimation of the crack-arrest capacity after the crack initiation is possible with the knowledge of the stress intensity factor K_I dependent on the component geometry and fault type or size.

6 References

[1] Winkler, H.-P.; Hüggenberg, R.; Ludwig, A.; Pusch, G.; Trubitz, P.: Determination and definition of fracture toughness of dynamically loaded ductile cast iron. 12th International Conference on Fracture, Juli 2009, Ottawa

[2] Ludwig, A.; Pusch, G.; Trubitz, P.; Winkler, H.-P.; Hüggenberg, R.: Ermittlung und Definition dynamischer Bruchzähigkeitswerte. Giesserei-Praxis 2012, Ausgabe 1/2, S. 10-13

[3] DYNTEST: Bestimmung dynamischer Rissinitiierungswerte für duktiles Gusseisen (DCI), Interner Bericht, TU Bergakademie Freiberg, Institut für Werkstofftechnik, 2008

[4] Baer, W.; Häcker, R.: Werkstoffcharakterisierung von Gusseisenwerkstoffen mit Kugelgraphit. MP Materialprüfung, 47 (2005) 1-2, S. 34-44.

[5] Rosenfield, A. R.; Ahmad, J.; Cialone, H. J.; Landow, M. P.; Mincer, P. N. and Papaspyropoulos, V.: Crack arrest toughness of nodular iron. In: Nuclear Engineering and Design 116 (1989), S. 161-170

[6] Gillot, R.: Experimentelle und numerische Untersuchungen zum Rissstopp-Verhalten von Stählen und Gusseisenwerkstoffen. Techn.-wiss. Ber. MPA Stuttgart (1988) Heft 88-03